Finite Element Analysis of Muscular Contractions from DC Pulses in the Liver

Long, G.L.[1*]PhD, Plescia, D.[1], Shires, P.K.[1] BVSc MS
[1]Ethicon Endo-Surgery, Cincinnati, Ohio
*Corresponding author: EES 4545 Creek Road, Cincinnati, Ohio, 45242 glong@its.jnj.com

Abstract:

Thermal ablation of malignant tumors has been conducted in patients who are not candidates for surgery for more than ten years[1]. Recently it has been shown that low energy DC pulses can cause cell necrosis. An undesirable characteristic of DC pulses in-vivo is the stimulation of skeletal muscle. The intensity of the contraction depends in part on the duration and height of the pulse. Through the use of Comsol Multiphysics, we have shown that the electrode design can affect the intensity of the contractions.

Keywords: Direct current pulses, muscle contractions, cell necrosis, tumor

1. Introduction

Direct current (DC) electric pulses have been shown to cause healthy liver cell necrosis in an in-vivo porcine model[2]. DC pulses with similar electrical parameters have also caused necrosis of human hepatocarcinoma cells (HepG2) in-vitro[3]. Destruction of malignant tumors with DC pulses may also be possible, but with the undesirable side effect of stimulation of adjacent skeletal muscle due to the high level of the exogenous field. While it is possible to inject paralytic agents such as pancuronium[4] to reduce the intensity of contractions, the procedure could then not be performed under conscious sedation.

We have made qualitative measurements in-vivo of muscle contractions with 2 different probe designs. The voltage level and the pulse duration affect the intensity of the contraction, but through the use of finite element analysis (Comsol Multiphysics), we have shown that the probe design also has an effect on the intensity of the contractions.

2. Background

The effects of electric fields on excitable tissue have been studied for many years beginning with Luigi Galvani's[5] publication in 1791. Excitation of skeletal muscle occurs when nerve impulses travel along mylenated nerve fibers which originate in the spinal cord[6]. The nerve impulse travels along the nerve axon and reaches the neuromuscular junction at which point acetylcholine is released. Each muscle fiber is covered by an excitable membrane with a resting potential of approximately 30-90 mV. The release of this excitory transmitter causes depolarization of the fiber membrane and a rapid contraction of the muscle[6]. If the nerve impulse is of a sufficiently high frequency, the muscle will not relax and a sustained contraction or tetanus occurs. Minimum tetanus frequencies range from 25 Hz to 60 Hz[7].

The action potentials of nerves have a duration of approximately 0.2 microseconds[8], while muscle action potentials durations are 1 to 5 milliseconds. When an external stimulus is applied to muscle it is the local nerves that are normally stimulated. Direct excitation of the muscle fibers is possible but requires pulses of longer duration and larger amplitude[7] than is required for nerves.

If an external stimulation or exogenous field is applied in the tissue, the magnitude and pulse width will affect the intensity of the muscular contraction. Rushton[9] showed that the orientation of the nerve with respect to the field will affect the excitation of the nerve. Furthermore the product of the characteristic length of the nerve, λ (the length such that the radial resistance of that length of membrane equals the longitudinal resistance of the inner core of the nerve axon) and the rate of change of the electric field d^2V/dx^2 determines the threshold of excitation[7, 9]. We define this quantity as ψ:

$$\psi = \lambda^2 * \frac{d^2V}{dx^2}$$

Equation 1

Where V is the voltage.

We will show that the number of electrodes and their separation as well as the distance to the

nerves affects the intensity of the contractions as well. We will confirm this with the results of our finite element model.

3. Methods

Three separate experiments were conducted with two probe designs. Probe A (Figure 1) had two 1 mm diameter needle electrodes (positive and ground) separated by 10 mm. Probe B (Figure 2) was constructed with two 0.5 mm diameter electrodes (positive) and two 1 mm diameter electrodes (negative). All applications (n=38) were made on live porcine liver through a laparotomy. The location of the probes on the liver was varied for each application. A metal pad was placed on the inside of the abdominal wall and connected to the ground electrode (N=4) to assess the effect of grounding the abdominal muscles, with the expectation that the muscles would not be depolarized by the pulses. Pulses were applied at 1500 VDC, 30 μsec (N=15) and 1500 VDC, 50 μsec (N=23). The intensity of each contraction was evaluated by the veterinary surgeon, and recorded (scale of 0 (none) to 5 (severe).

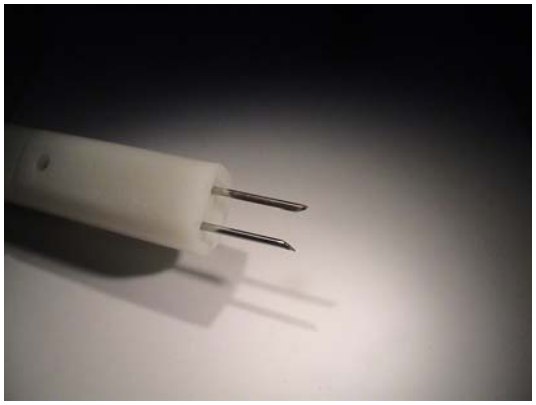

Figure 1. Probe A, one positive and negative electrode.

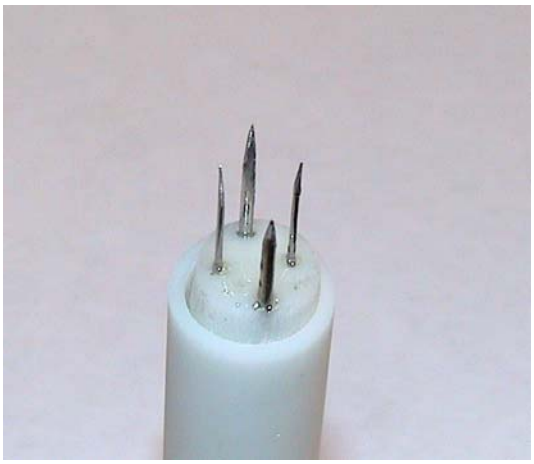

Figure 2. Probe B, two positive and two negative electrodes.

A finite element model was created for each probe, with and without the ground pad, on homogeneous liver tissue. The electric field and voltage were then plotted from the solutions of the models.

The specimens were harvested and processed for histopathological examination. The electric field solution was aligned with a digital image of the histological slide to determine an electric field threshold of cell necrosis.

4. Finite Element Model

A three dimensional Finite Element (FE) model was created and analyzed using Comsol Multiphysics (Comsol, MA, USA). The electrodes were embedded in a subdomain, which represented a homogeneous section of liver. Figure 3 is the mesh for probe A. The model contained 12,004 elements and 24,281 degrees of freedom (DOF). The model for probe B contained 15,098 elements and 30,581 DOF.

Three application modes were used to solve the problem; conductive media DC and two PDE, general form modes. To calculate the electric field strength, the Laplace equation was solved (static electric field):

$$\nabla \bullet \left(\sigma \nabla V \right) = 0$$

Equation 2

Where σ is tissue conductivity and V is the voltage. The value for tissue conductivity depends on both the temperature of tissue[10] and the electric field strength[11]. It has been shown that the temperature increase is negligible[12], therefore the temperature dependence was ignored.

When modeling the electric field strength for the DC pulses, an electric field strength dependent σ is used[13]:

$$\sigma(E) = (E_2, \sigma_2, if(E_1, \sigma_1, \sigma_0))$$

Equation 3

Where σ2 and σ1 are set when E1 and E2 are reached in the tissue. The initial value for conductivity is σ0. Equation 1 is entered as the value for electrical conductivity in the conductive media application mode. The PDE modes are used as logic functions to test whether the electric field threshold has been reached.
The problem is solved in iterations. The first solution is obtained with σ0. The problem is then solved with "restart" until the solution reaches steady state. Our values for electrical conductivity were σ0=0.1S/m and σ1=0.15S/m. The excitation threshold, ψ was plotted in the model by entering equation 1 in expression box of the cross section plot parameters.

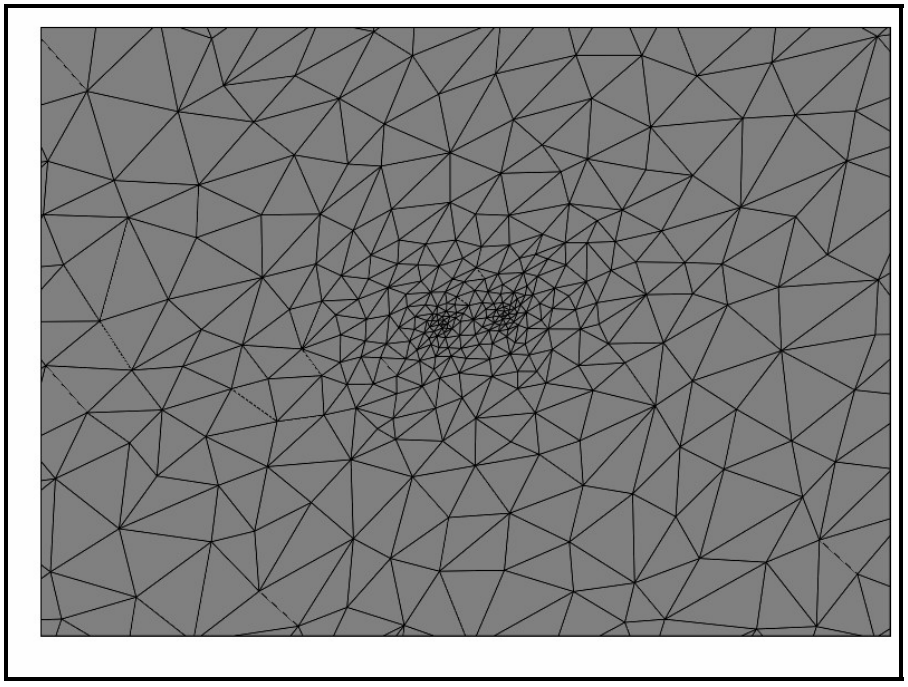

Figure 3. Three dimensional model of probe A in tissue with mesh. The electrodes were subtracted from the tissue subdomain to create conductive surfaces.

5. Results

The most severe contractions occurred when the ground pad was placed on the tissue (mean= 4.7, n=3). With the ground pad applications removed from the data, there was a significant difference in the mean contraction score of Probe A and B (mean=2.35, 0.78 p=0.005, n=17, 18). The FEA showed that the voltage across the liver remains at a relatively high level (with respect to the ground electrode), with the exception of the ground pad solution (Figure 7).

Figures 4 and 5 are isosurface plots of the electric field for probe A and B respectively at a value of 800V/cm.

Figure 6 is a statistical plot of the contractions of each probe.

Figure 7 is a line plot of each probe. The four plots included are; probe A, probe A with ground, and probe B along the positive electrodes and the negative electrodes.

Figures 8 and 9 are line plots of ψ.

Figure 10, 11 and 12 are surface plots of ψ.

Figure 13 is a photograph of a section of the liver which had pulses applied by probe B. The speciman was stained with a dye that is taken up by viable cells and not by dead cells. Therefore, the purple section is live cells and the white section contains dead cells. The electric field solution was aligned with the photograph of the slide. The solution ranges from 500V/cm to 900V/cm.

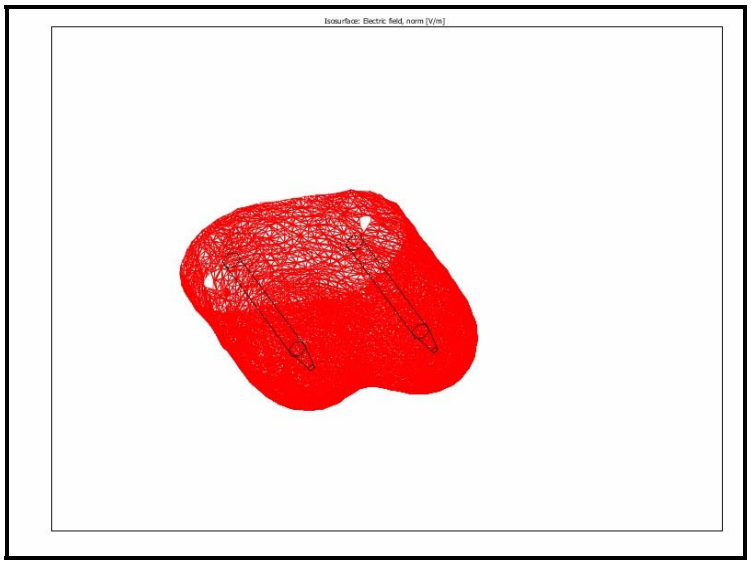

Figure 4. Surface plot of the electric field produced by probe A at 1500 Vdc excitation.

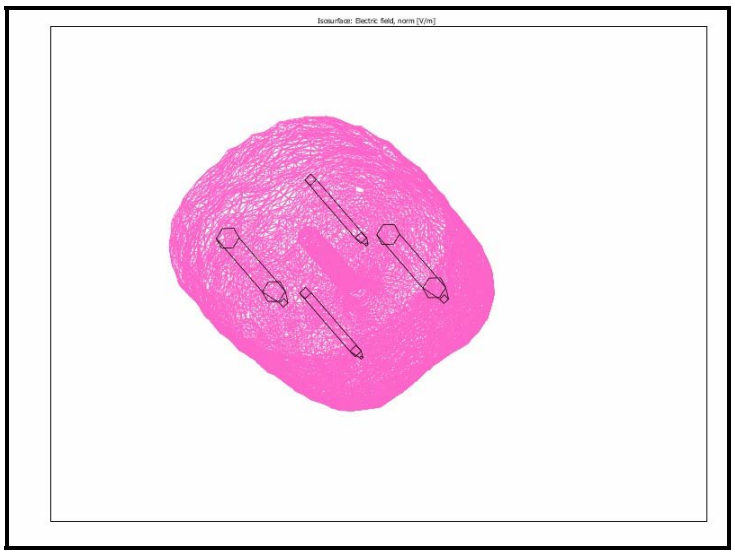

Figure 5. Surface plot of the electric field produced by probe B. The field drops to a local minimum in the center.

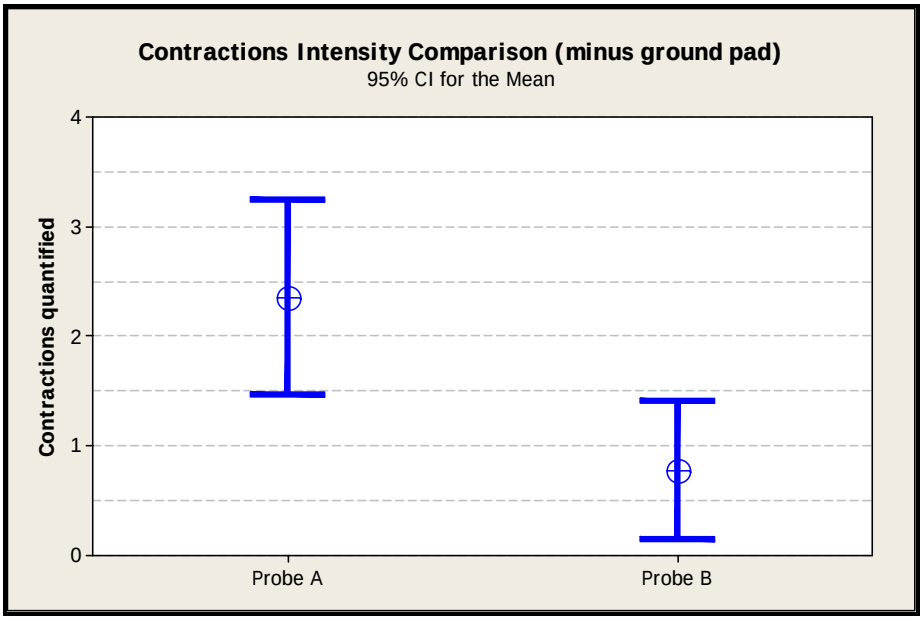

Figure 6. Plot of the intensity of the contractions for each probe. The data for the ground pad were removed.

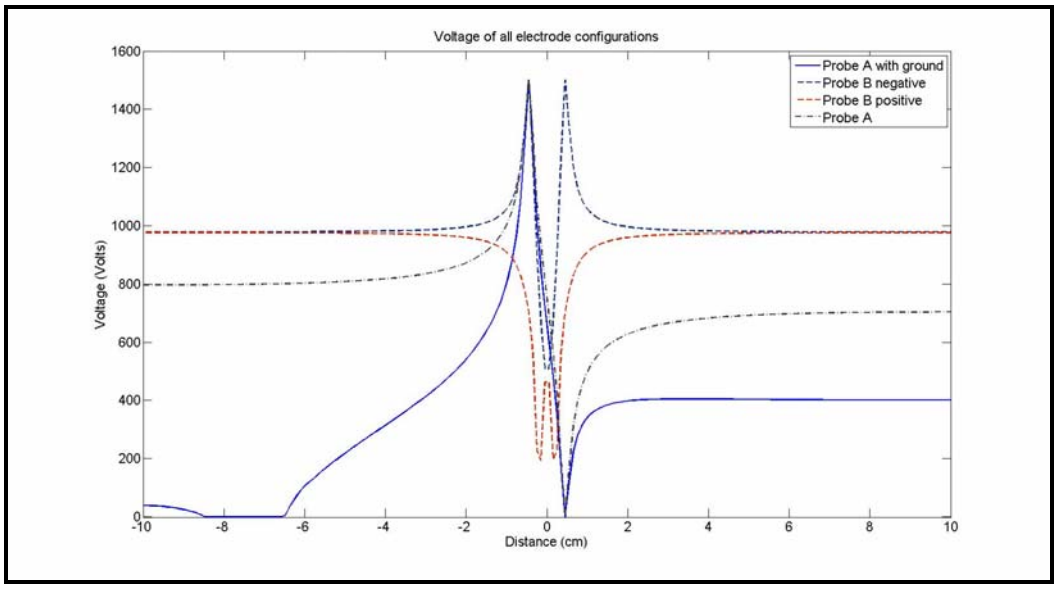

Figure 7. Line plot of voltage for all probes along the tissue.

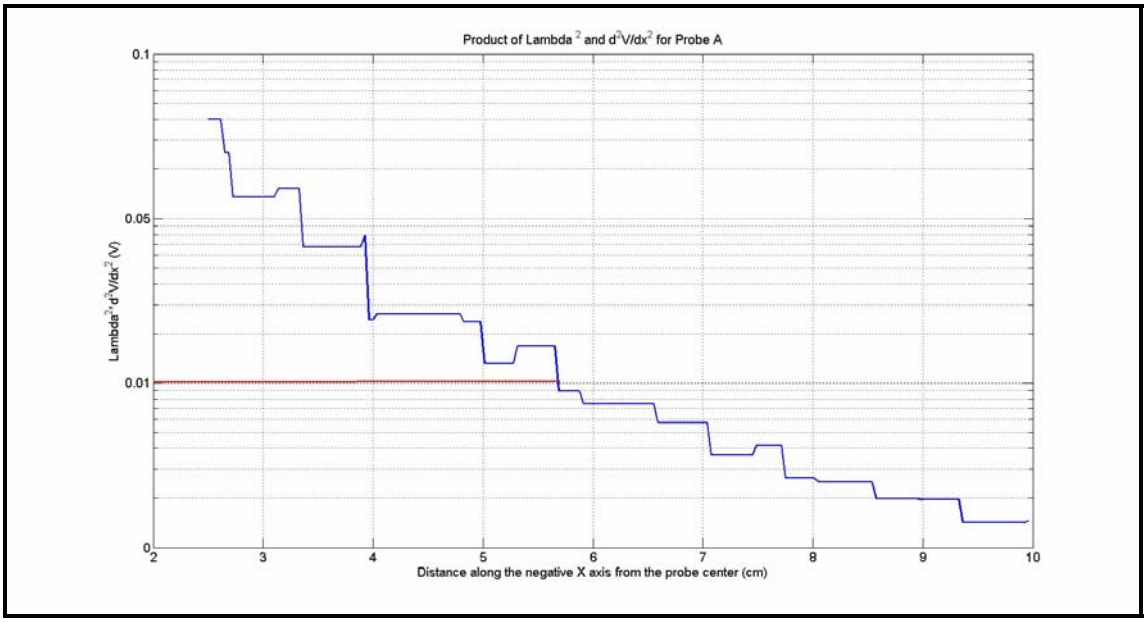

Figure 8. Line plot of ψ from 2.5cm to 10cm from probe A.

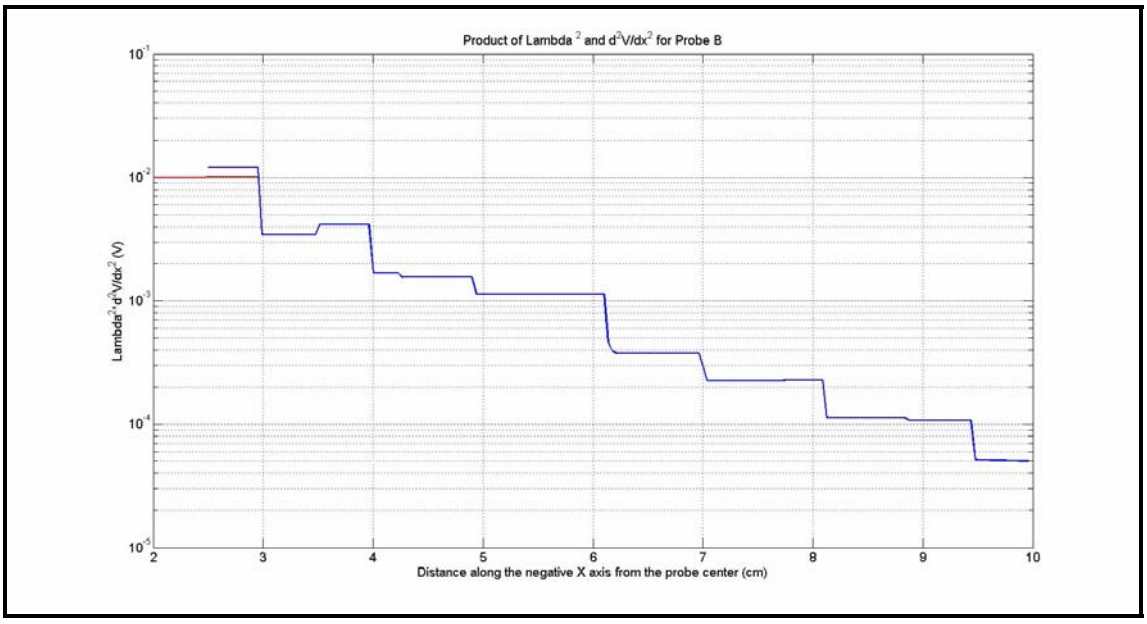

Figure 9. Line plot of ψ from 2.5cm to 7 cm on a diagonal from probe B.

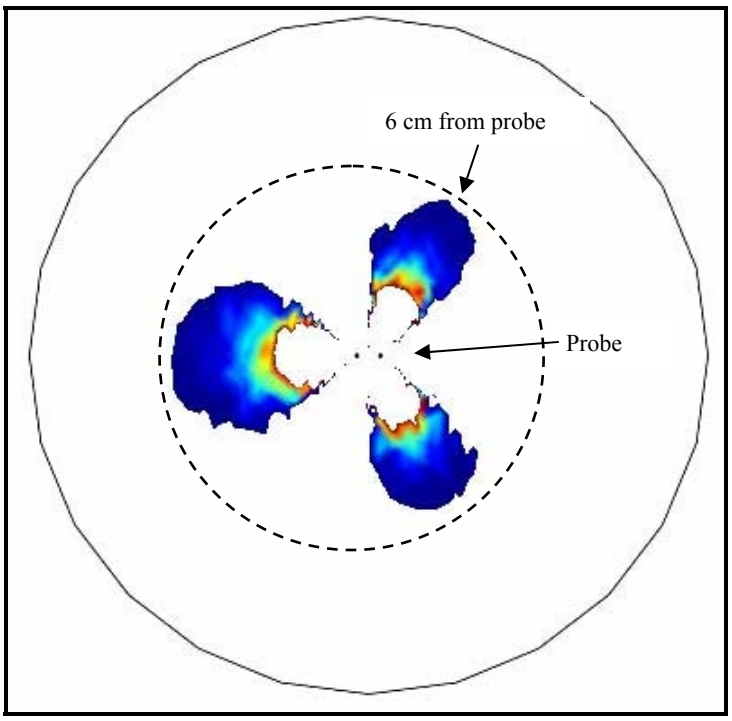

Figure 10. Surface plot of ψ for probe A. The color zones ranges from 0.01V (threshold) to 0.2V.

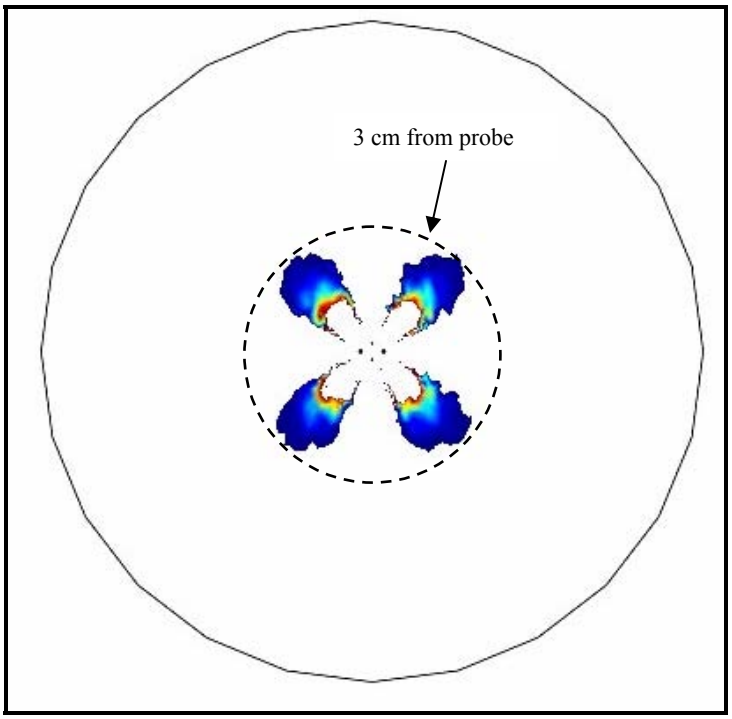

Figure 11. Surface plot of ψ for probe A. Any nerves outside this zone will not be stimulated.

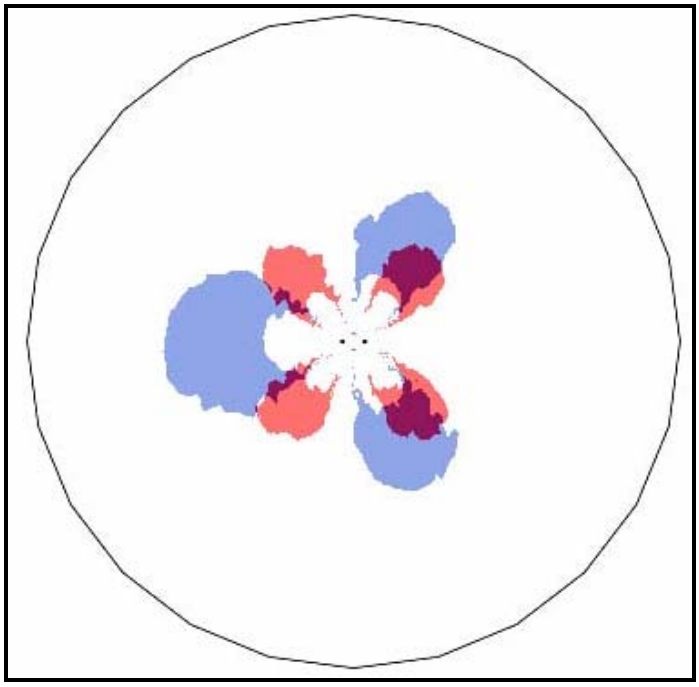

Figure 12. Comparison ψ for probe A and probe B.

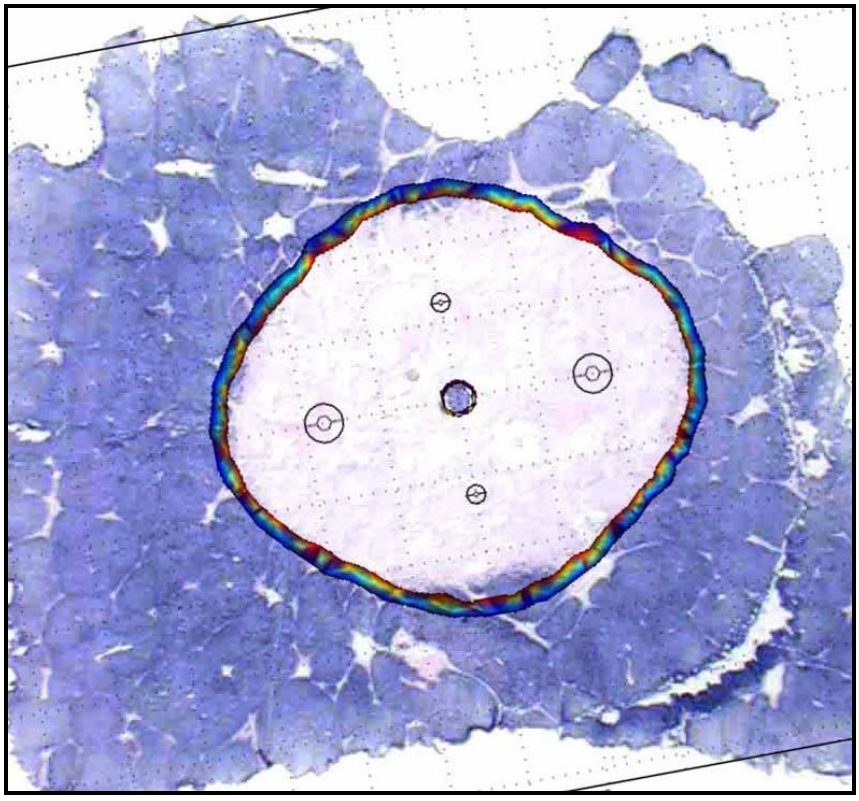

Figure 13. Pathology slide with model overlay.

6. Discussion

According to Guyton[14] an increase of 0.140 VDC in the end plate potential is required for excitation of skeletal muscle. While these magnitudes may be high enough to directly stimulate the muscle, it is unlikely because, as already mentioned, Lale[7] reported that longer pulse widths would be required.

According to Lale[7], the threshold of excitation of a nerve is ψ= 10 mV. The difference in thresholds of probe A and B can be seen graphically in Figures 8 and 9. The value of ψ falls below the threshold value of 10mV at 6cm and 3cm for probes A and B respectively. If a procedure were performed laparoscopically, the liver would be separated from the abdominal muscle due to the pressurized abdominal cavity. The distance from the central liver of the pig to the abdominal muscles is on the order of 10 cm. Therefore the further reaching zone of probe A would likely cause more severe contraction. Since ψ falls off exponentially, the contractions will become quite severe as the probe is placed near the abdominal wall e.g. placing the probe in a lateral lobe.

Ψ was plotted in Comsol to determine the threshold of contraction. Figures 10 and 11 were generated by typing the equation for ψ in the expression box of the *post process cross-section plot parameters* menu. The plots range from 2.5 cm to 10 cm.

Ψ was then entered in the expression box of the *surface plot* in the post-processing menu to graphically illustrate the zones where contractions will occur (Figures 12 and 13).

When the electric field solution was aligned with the pathology slide (Figure 13), the necrotic threshold is approximately 700- 800 V/cm which agrees well with the value of 637 +/- 43 V/cm reported by Miklavcic[2]. Notice that the model predicts that the cells would not be killed at the local minima of the electric field in the center of the treatment zone.

7. Conclusion

The electrode configuration does affect the intensity of muscular contractions in-vivo. The substantial increase in distal voltage drop when a ground pad is attached seems to explain the severity of contractions when the pad is used as opposed to the expected reduction of contraction intensity.

While the model demonstrated a difference in the voltage drop 10 cm distal to the probes, it is the rate of change of the electric field with respect to space (ψ) that stimulates the nerves and causes muscular contractions. Through the use of Comsol Multiphysics, we have shown that the threshold of contraction of this value extends further with probe A as compared to probe B.

The limitation of the model is the heterogeneity of the liver as well not knowing precisely which muscle contracted. This information would allow us to place the anatomical location of the nerves and muscles in the model and perform a more thorough analysis.

The next steps are to measure potentials in-vivo to validate the model and conduct experiments designed to perform a more rigorous statistical analysis.

Reference List

1. Abitabile P, Hartl U, Lange J, Maurer CA. Radiofrequency ablation permits an effective treatment for colorectal liver metastasis. European Journal of Surgical Oncology 2007;33:67-71.

2. Miklavcic D, Semrov D, Mekid H, Mir LM. A validated model of in vivo electric field distribution in tissues for electrochemotherapy and for DNA electrotransfer for gene therapy. Biochim Biophys Acta 2000;1523:73-83.

3. Miller L, Leor J, Rubinsky B. Cancer cells ablation with irreversible electroporation. Technol Cancer Res Treat 2005;4:699-705.

4. Onik G, Mikus P, Rubinsky B. Irreversible electroporation: implications for prostate ablation.

Technol Cancer Res Treat 2007;6:295-300.

5. Piccolino M. Visual images in Luigi Galvani's path to animal electricity. J Hist Neurosci 2008;17:335-348.

6. Guyton AC, Hall JE. Contraction of Skeletal Muscle. Textbook of Medical Physiology. 2000:82-84.

7. Lale PG. Muscular contraction by implanted stimulators. Med Biol Eng 1966;4:319-331.

8. Guyton AC, Hall JE. Membrane Potentials and Action Potentials. In: W.B.Sanders, ed. Textbook of Medicle Physiology. 2000:56.

9. Rushton WA. The effect upon the threshold for nervous excitation of the length of nerve exposed, and the angle between current and nerve. J Physiol 1927;63:357-377.

10. Chang I. Finite Element Analysis of Hepatic Radiofrequency Ablation Probes using Temperature-Dependent Electrical Conductivity. Biomed Eng Online 2003;2:12.

11. Miklavcic D, Pavselj N. Electrical Properties of Tissue. Elkectroporation Based Technologies and Treatments 7 A.D.;13-18.

12. Edd JF, Horowitz L, Davalos RV, Mir LM, Rubinsky B. In vivo results of a new focal tissue ablation technique: irreversible electroporation. IEEE Trans Biomed Eng 2006;53:1409-1415.

13. Pavselj N, Bregar Z, Cukjati D, Batiuskaite D, Mir LM, Miklavcic D. The course of tissue permeabilization studied on a mathematical model of a subcutaneous tumor in small animals. IEEE Trans Biomed Eng 2005;52:1373-1381.

14. Guyton, Hall. Excitation of skeletal muscle. Textbook of Physiology. 2000:82.